COMMUNICATION

ChemComm
www.rsc.org/chemcomm

Pore size effects in the pyrolysis of 1,3-diphenylpropane confined in mesoporous silicas

Michelle K. Kidder, Phillip F. Britt, Zongtao Zhang, Sheng Dai and A. C. Buchanan, III*
Chemical Sciences Division, Oak Ridge National Laboratory, Bethel Valley Road, Oak Ridge, Tennessee, USA 37831-6197. E-mail: buchananac@ornl.gov

Received (in Corvallis, OR, USA) 27th August 2003, Accepted 23rd September 2003
First published as an Advance Article on the web 15th October 2003

A new method for derivatizing mesoporous silicas, SBA-15 and MCM-41, with a substituted phenol is described, and pore confinement and surface curvature are shown to impact the reaction rate and product selectivity for the pyrolysis of surface-immobilized 1,3-diphenylpropane.

Ordered mesoporous silicas continue to receive enormous attention owing to their many potential applications such as in catalysis and selective separations.[1] The pore surfaces of these high surface area materials are readily functionalized typically by reaction of the silanols with silane coupling agents such as silyl chlorides, silyl alkoxides, and disilazanes, which result in siloxane linkages (Si–O–Si) to the surface.[2–5] In this communication, we report a different method for functionalizing mesoporous silicas utilizing a phenol functional group as the coupling agent, which establishes a silyl ether linkage (Si–O–C$_{aryl}$) to the surface. The principal advantage of this linkage is that it is thermally robust permitting the study of reactions at high temperature, yet it is easily cleaved with aqueous base so that surface bound products are readily retrieved. This is illustrated through the study of the pyrolysis of surface-immobilized 1,3-diphenylpropane (DPP) at 375 °C. In addition, the effect of pore size (5.6–1.7 nm) of mesoporous silica on the maximum achievable DPP surface coverage is examined, as well as the impact of pore confinement and size on the DPP pyrolysis rate and product selectivity.

Hexagonal mesoporous silicas were synthesized by standard methods,† and their surface areas and pore sizes, determined from nitrogen sorption isotherm measurements, are listed in Table 1. Saturation surface coverages of DPP on the silicas were prepared by reaction of the surface silanols with an excess of *p*-(3-phenylpropyl)phenol (HODPP) as shown in Fig. 1.† BET analysis of a MCM-41 (1088 m^2 g^{-1}, 2.9 nm) derivative gave an isotherm with a lower surface area (619 m^2 g^{-1}) and mean pore diameter (1.6 nm) as expected. The coverages are reported in Table 1 along with the surface densities, which are normalized for the differences in the silica surface areas. The results are compared with those obtained for Cabosil, a nonporous fumed silica. It is immediately seen that the saturation surface densities of DPP are lower for the porous materials (0.96–1.37 nm^{-2}) than for the nonporous Cabosil. The trend for the three structurally analogous MCM-41s shows that the maximum surface density for DPP decreases with decreasing pore size, a result of steric crowding. Interestingly, derivatization of the SBA-15 (5.6 nm) gives a lower DPP surface density than for the MCM-41 (2.9 nm) despite the larger pore size. This is likely a consequence of the fact that SBA-15 has a significant amount of its surface area in micropores that interconnect the mesopores and may not be accessible to the DPP molecules.[5,6] This effect is also observed to a smaller extent for a smaller SiMe$_2$H derivative described below (Table 1).

For comparison, the silicas were also silylated with 1,1,3,3-tetramethyldisilazane according to the procedure of Anwander *et al.*,[4] and the results are given in Table 1. Our value for silylation of the 2.9 nm MCM-41 of 1.99 silyl groups nm^{-2} agrees favorably with that obtained by Anwander for a related MCM-41 sample with a slightly higher surface area of 1139 m^2 g^{-1} (1.85 nm^{-2}). We observe that as the pore size of the MCM-41 silica decreases (2.9–1.7 nm), the degree of silylation also decreases following the same trend as for DPP. Anwander has recently observed similar behaviour for silylation of the cubic phase MCM-48 over the pore size range of 3.8–1.6 nm, and attributed the effect to increasing pore surface curvature at the smaller pore sizes resulting in steric crowding.[5] We note that the smaller degrees of derivatization of the silicas (including the Cabosil) with DPP compared to the Si(CH$_3$)$_2$H moieties is consistent with the larger size of the DPP group.

Pyrolysis of DPP at 375 °C in the gas phase[7] or attached to the surface of Cabosil[8] occurs by a free-radical chain reaction to produce toluene and styrene as the major products.‡ The radical chain propagation steps on a surface involve hydrogen abstraction by both surface-attached and gas-phase benzyl radicals from the benzylic positions of DPP to give regiochemically distinct benzylic radicals, which undergo facile β-scission to produce the surface-attached and gas-phase styrene products, as well as regenerating the chain-carrying benzyl radicals.[8] For DPP attached to the surface of the SBA-15 and MCM-41 silicas, the same two pairs of products are formed as was observed on the nonporous Cabosil (Fig. 2). Even for the smallest pore diameter MCM-41 (1.7 nm) investigated, where DPP molecules

Table 1 Properties of derivatized silica surfaces and pyrolysis data for immobilized 1,3-diphenylpropane at 375 °C

Silica	Surface area[a]/ m^2 g^{-1}	Pore diameter[b]/ nm	SiMe$_2$H coverage[c]/ mmol g^{-1}	SiMe$_2$H density[d]/ nm^{-2}	DPP coverage[e]/ mmol g^{-1}	DPP density[d]/ nm^{-2}	Rxn. rate[f] at 375 °C (% h^{-1})	Product selectivity PhVi : PhMe[g]
Cabosil	200	n.a.	0.68	2.12	0.54	1.82	8.4[h]	0.95[h]
SBA-15	867	5.6	2.26	1.81	1.17	1.05	12.2	1.04
MCM-41	1088	2.9	2.97	1.99	1.67	1.37	14.4	1.08
MCM-41	1194	2.2	2.35	1.38	1.56	1.13	17.5	1.14
MCM-41	1285	1.7	1.92	1.00	1.46	0.96	16.8	1.14

[a] From the BET nitrogen adsorption isotherm. [b] BJH mean pore diameter calculated from the desorption branch. [c] Surface coverage from carbon elemental analysis measured per gram of derivatized silica. [d] Molecular density (molecules per nm^2 surface area) corrected for the weight of the organic moiety. [e] Average of the surface coverages obtained from chemical analysis (see text) and carbon elemental analysis (error is ±3%). [f] Initial pyrolysis rate measured from the slope (linear regression) of a plot of percentage diphenylpropane conversion (limited to 15% maximum) *versus* reaction time; typical error is ±5–10%. [g] Reaction path selectivity measured by the styrene (PhVi) to toluene (PhMe) product yield ratio (error is ±2%). [h] From Buchanan *et al.*[8]

DOI: 10.1039/b310405b

(*ca* 1.2 nm in length) could potentially become entangled, no new products were detected and mass balances were quantitative (±5%).

Surprisingly, the pyrolysis rates for DPP attached to the mesoporous silicas are all 1.5–2.0-fold faster than for DPP on the nonporous Cabosil (Table 1) despite the smaller densities of surface-bound molecules at saturation coverage. Previously, pyrolysis rates for DPP on Cabosil were found to decrease rapidly at lower densities of DPP molecules on the surface, since the rates of propagating hydrogen transfer steps, particularly on the surface, are greatly diminished.[8] For example, decreasing the DPP surface density on Cabosil from 1.82 to 0.43 nm^{-2} resulted in a 20-fold decrease in the pyrolysis rate. Hence, pore confinement results in a more efficient radical chain decomposition reaction for DPP. This could result from enhanced encounter frequencies and improved geometries for hydrogen transfer to gas-phase and surface-attached benzyl radicals in the pores. It is also interesting that the rates for the 1.7 and 2.2 nm MCM-41 samples are about 40% larger than for the 5.6 nm SBA-15 sample at comparable surface densities of 1.0–1.1 DPP nm^{-2}, indicating that confinement of DPP in the smaller pores leads to faster rates.

Selectivity in product formation is determined by the relative rates of hydrogen abstraction at the two distinct benzylic methylene sites, since the rate of subsequent β-scission steps for the resulting radicals is fast.[7,8] This selectivity is measured by the ratio of styrene to toluene product yields, which arise from β-scission of $\equiv$SiOPhCH$_2$CH$_2$C$^{\cdot}$HPh (**1**) and $\equiv$SiOPhC$^{\cdot}$HCH$_2$CH$_2$Ph (**2**) radicals, respectively. For Cabosil, the selectivity was 0.95 consistent with a small substituent effect ($\equiv$SiO–) favoring formation of **2**.[8] Interestingly, the selectivity values for the mesoporous silicas are all greater than 1.0 (Table 1) and tend to increase with decreasing pore size (and increasing pore surface curvature). This indicates that the benzylic methylene hydrogens farthest from the surface, leading to radical **1**, are becoming more accessible for hydrogen abstraction by benzyl radicals as illustrated in Fig. 3 for the surface radical.

These studies have shown that mesoporous silicas are readily derivatized by aromatic phenols to give hybrid materials possessing silyl aryl ether linkages. Significantly, pore confinement is shown to impact both the reaction rate and product selectivity for a free-radical reaction, and these effects are magnified at smaller pore sizes.

This research was sponsored by the Division of Chemical Sciences, Geosciences, and Biosciences, Office of Basic Energy Sciences, US Department of Energy under contract DE-AC05-00OR22725 with Oak Ridge National Laboratory, managed and operated by UT-Battelle, LLC.

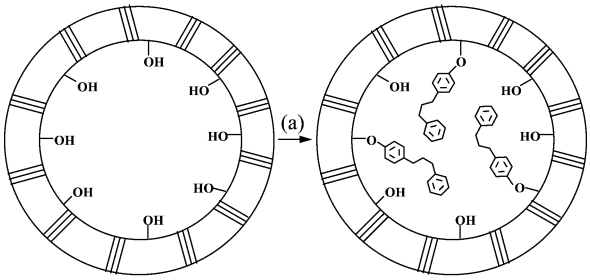

Fig. 1 Preparation of 1,3-diphenylpropane (DPP) immobilized in mesoporous silicas with a Si–O–C$_{aryl}$ linkage. (a) Silanols are condensed with *p*-HOPh(CH$_2$)$_3$Ph at 225 °C under vacuum.

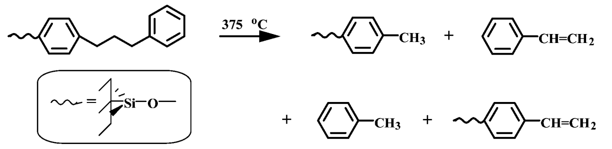

Fig. 2 Gas-phase and surface-attached products from pyrolysis of DPP immobilized on mesoporous silicas.

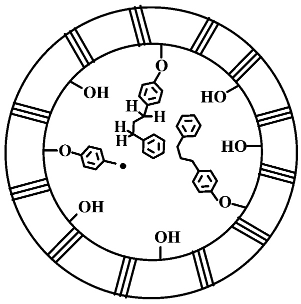

Fig. 3 Illustration of potential regioselectivity in hydrogen abstraction by surface-attached benzyl radicals based on accessibility of the benzylic methylene sites of pore-confined DPP.

Notes and references

† Mesoporous silicas were synthesized following the procedures described by Jarupatrakorn and Tilley.[9] The three MCM-41 samples of 2.9, 2.2, and 1.7 nm pore size were prepared utilizing $C_nH_{2n+1}N(CH_3)_3Br$ [n = 16, 14, 12, respectively] as structure directing templates. A typical surface attachment reaction for the MCM-41 sample with a surface area of 1088 m^2 g^{-1} involved adsorption of *p*-(3-phenylpropyl)phenol (HODPP; 2.7 g, 12.7 mmol) onto the surface of the silica (1 g, *ca.* 4.6 mmol SiOH assuming a maximum of 2.5 SiOH nm^{-2} derivatizable[3–5]), which had been dried at 200 °C for 4 h, by solvent evaporation from a benzene slurry. The attachment reaction was performed at 225 °C for 1 h in a fluidized sand bath on a degassed, evacuated ($< 10^{-5}$ Torr), sealed sample. The sample was transferred to another tube, connected to a vacuum at 5×10^{-3} Torr, heated in a tube furnace from 225 to 275 °C at a rate of 10 °C min^{-1}, and held at 275 °C for 10 min to remove unattached HODPP. The samples were stored in a desiccator under vacuum. Surface coverage analysis involved base hydrolysis of a sample (1 M NaOH), addition of *p*-phenylphenol as internal standard, acidification with HCl, extraction with CH$_2$Cl$_2$, drying over MgSO$_4$, and solvent evaporation. The residue was silylated with *N*,*O*-bis(trimethylsilyl)trifluoroacetamide : pyridine (1 : 2) and analyzed *via* GC using a J & W Scientific 30 m × 0.25 mm id, 0.25 μm film thickness DB-5 column and flame-ionization detection. Chemical purities of the recovered DPP moieties by GC analysis were $> 99.5\%$. The surface coverage was also independently verified by carbon elemental analysis (Galbraith Laboratories).

‡ A weighed amount of sample (50–90 mg) was placed in one end of a T-shaped Pyrex tube, evacuated, and sealed at *ca.* 2×10^{-6} Torr. The sample was inserted into a preheated temperature-controlled, three-zone tube furnace (±1 °C) fitted with a copper sample holder, and the other end was placed in a liquid nitrogen bath. The products that evolved into the gas phase were collected in the cold trap and dissolved in acetone (0.1–0.2 mL) along with internal quantification standards. These products were analyzed by GC and GC-MS (70 eV). The surface-attached products were analyzed similarly following base hydrolysis of the solid residue analogous to the surface coverage analysis procedure described above.

1 J. M. Thomas, B. F. G. Johnson, R. Raja, G. Sankar and P. A. Midgely, *Acc. Chem. Res.*, 2003, **36**, 20; H. P. Lin and C.-Y. Mou, *Acc. Chem. Res.*, 2002, **35**, 927; D. Brunel, A. C. Blanc, A. Galarneau and F. Fajula, *Catal. Today*, 2002, **73**, 139.
2 A. Stein, B. J. Melde and R. C. Schroden, *Adv. Mater.*, 2000, **12**, 1403.
3 R. Anwander, *Chem. Mater.*, 2001, **13**, 4419.
4 R. Anwander, I. Nagl, M. Widenmeyer, G. Engelhardt, O. Groeger, C. Palm and T. Roser, *J. Phys. Chem. B*, 2000, **104**, 3532.
5 M. Widenmeyer and R. Anwander, *Chem. Mater.*, 2002, **14**, 1827.
6 S. H. Joo, R. Ryoo, M. Kruk and M. Jaroniec, *J. Phys. Chem.*, 2002, **106**, 4640; A. Galarneau, H. Cambon, F. Di Renzo, R. Ryoo, M. Choi and F. Fajula, *New J. Chem.*, 2003, **27**, 73.
7 M. L. Poutsma and C. W. Dyer, *J. Org. Chem.*, 1982, **47**, 4903; K. E. Gilbert and J. J. Gajewski, *J. Org. Chem.*, 1982, **47**, 4899.
8 A. C. Buchanan, III, P. F. Britt, K. B. Thomas and C. A. Biggs, *J. Am. Chem. Soc.*, 1996, **118**, 2182; A. C. Buchanan, III and C. A. Biggs, *J. Org. Chem.*, 1989, **54**, 517.
9 J. Jarupatrakorn and T. D. Tilley, *J. Am. Chem. Soc.*, 2002, **124**, 8380.